Supplemental information

Needle biopsy accelerates pro-metastatic changes and systemic dissemination in breast cancer: Implications for mortality by surgery delay

Hiroyasu Kameyama, Priya Dondapati, Reese Simmons, Macall Leslie, John F. Langenheim, Yunguang Sun, Misung Yi, Aubrey Rottschaefer, Rashmi Pathak, Shreya Nuguri, Kar-Ming Fung, Shirng-Wern Tsaih, Inna Chervoneva, Hallgeir Rui, and Takemi Tanaka

Supplementary Information

Needle biopsy accelerates pro-metastatic changes and systemic dissemination in breast cancer: Implications for mortality by surgery delay

Hiroyasu Kameyama, Priya Dondapati, Reese Simmons, Macall Leslie, John F. Langenheim, Yunguang Sun, Misung Yi, Aubrey Rottschaefer, Rashmi Pathak, Shreya Nuguri, Kar-Ming Fung, Shirng-Wern Tsaih, Inna Chervoneva, Hallgeir Rui, and Takemi Tanaka

Lead Contact:

Takemi Tanaka, Ph.D., Professor
University of Oklahoma Health Sciences Center, School of Medicine, Dept. of Pathology, Stephenson Cancer Center at 975 NE 10th St, BRC-W, Rm 1415, Oklahoma City, OK 73104
Email: takemi-tanaka@ouhsc.edu
Phone: Office (405)-271-8260

This PDF included Figure S1-S7 and Table S1-S4

Figure S1

A

Py230^{mCherry}

Brightfield   Fluorescence

Py2T^{mCherry}

Brightfield   Fluorescence

100 μm   100 μm   100 μm   100 μm

B

Py230^{mCherry} Tumor (15-day post-biopsy)

Adjacent   Distant

Py2T^{mCherry} Tumor (15-day post-biopsy)

Adjacent   Distant

BW   200 μm   200 μm   BW   200 μm   200 μm

Brown: anti-mCherry   Blue: hematoxylin

C

Py230^{mCherry} (B6)

Gate   Tumor volume

Biopsy(+)   Biopsy(−)

TxRed   FITC

Body weight

Py2T^{mCherry} (FVB)

Gate   Tumor volume

Biopsy(+)   Biopsy(−)

TxRed   FITC

Body weight

D

Py230^{mCherry}   30 days   Biopsy   6 hours   Whole Blood collection for FACS

WBC   Py230^{mCherry}   Py230^{mCherry}   WBC

TxRed   FITC

mCherry+ cells in blood (count)   Biopsy   −   +

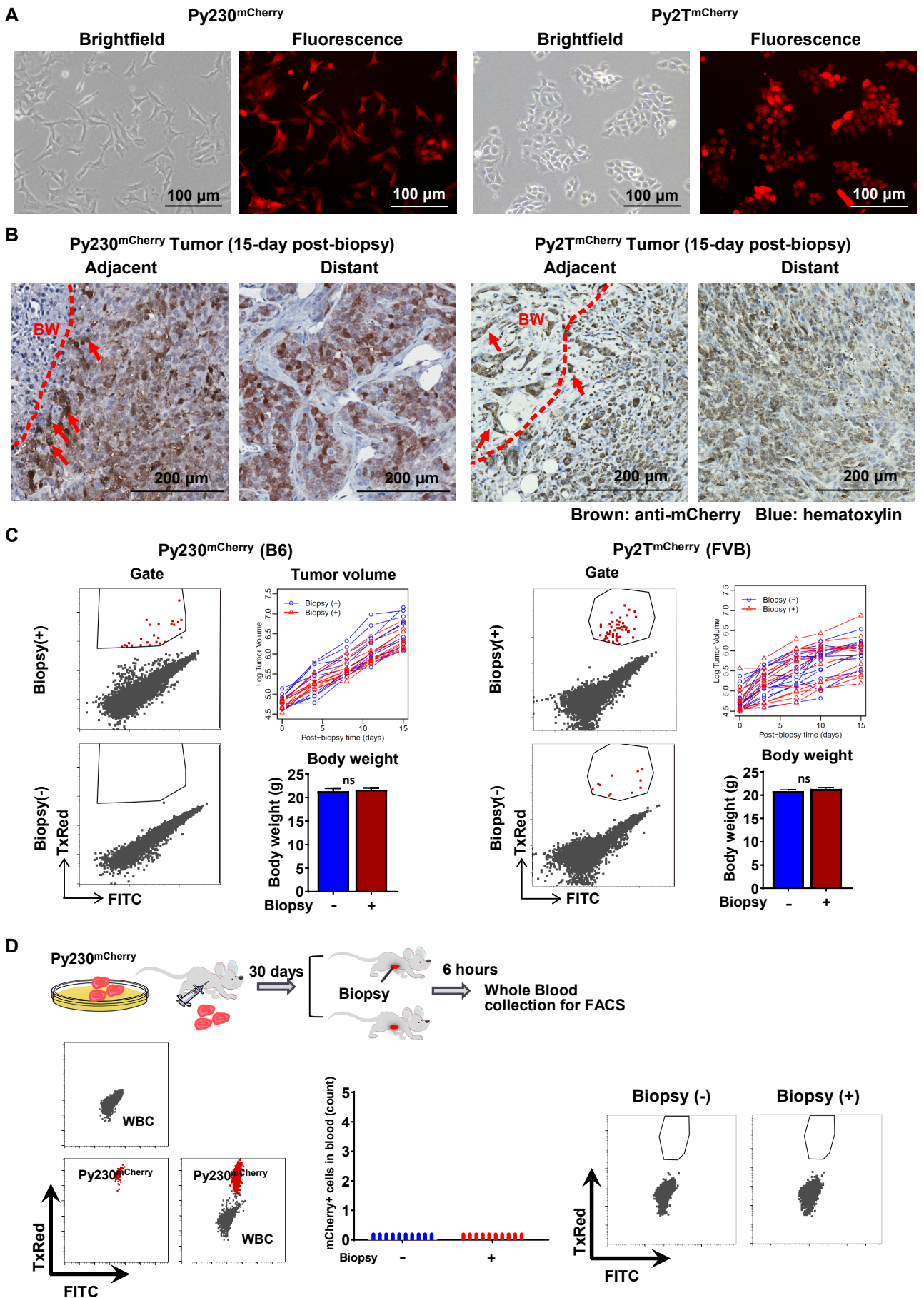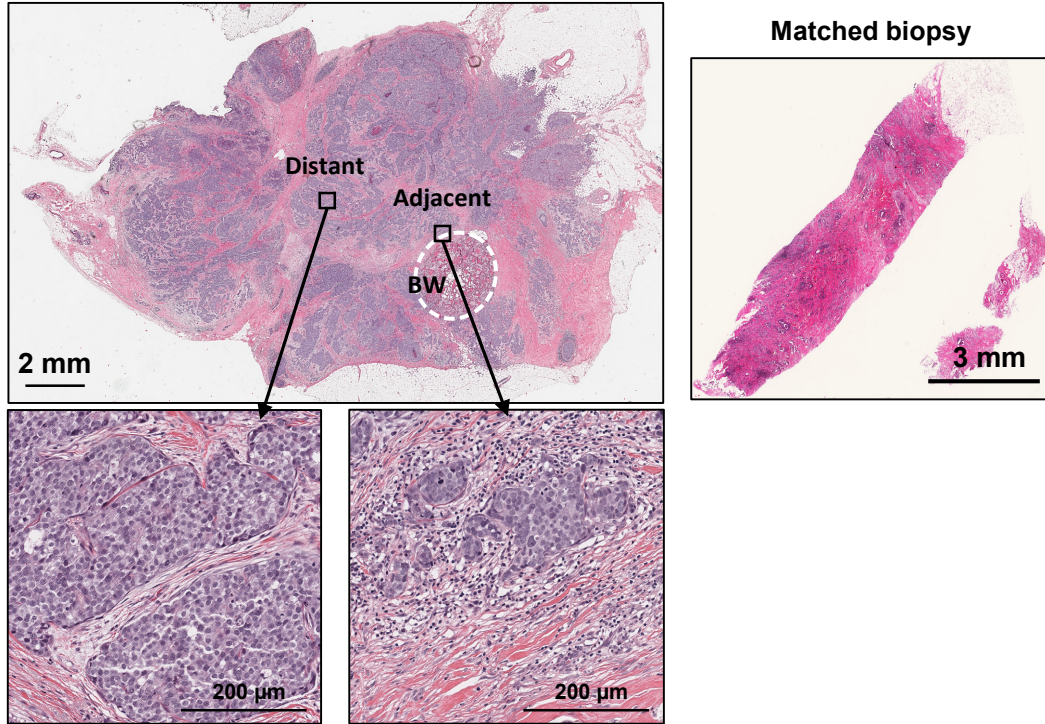Biopsy (−)   Biopsy (+)

TxRed   FITC

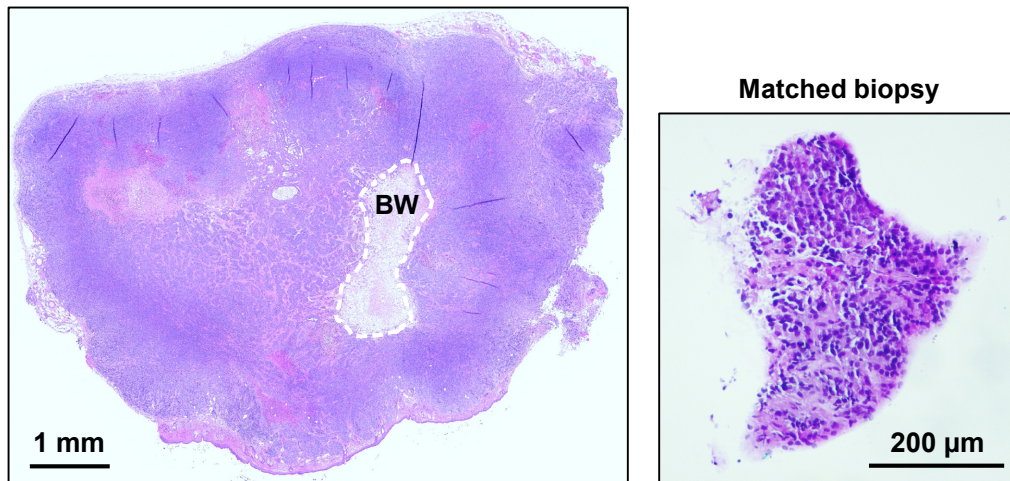**Figure S1. Needle biopsy of breast tumor does not cause cancer cell displacement, related to Figure 1.**
(A) Brightfield and fluorescent images of Py230^{mCherry} and Py2T^{mCherry} mouse mammary carcinoma cells. (B) Immunohistochemical staining of mCherry (brown) in 15-day post-biopsy Py230^{mCherry} and Py2T^{mCherry} tumors both adjacent (left) to and distant (right) from biopsy wound. The slides were counterstained with Hematoxylin (blue). Red arrows indicate spindle-shaped mCherry+ cancer cells adjacent immediately outside of the wound; the red dotted line indicates the boundary of the biopsy wound. BW: biopsy wound. (C) Representative images of flow cytometric analyses of mCherry-positive BC cells after scatter gating and live cell gating of whole lung of Py230^{mCherry} and Py2T^{mCherry} tumors. The growth rate of Py230^{mCherry} and Py2T^{mCherry} tumors derived from mice assigned to study in Figure 1E (n=10-13) and 1F (n=11-12), respectively. Tumor volume of each mouse was plotted over post-biopsy days (biopsy as day 0); *P*-values were calculated using Student's T-test. The endpoint bodyweight of the mice assigned to this study; *P*-values were calculated using Student's T-test. (D) The absence of disseminated Py230^{mCherry} cells in the circulation after tumor biopsy. Whole blood was collected from B6 mice by cardiac puncture 6 hours following biopsy of the Py230^{mCherry} tumor. Following red blood cell lysis, a single cell suspension of white blood cells (WBCs) was analyzed by flow cytometry (n=10). Flow cytometry gating shows WBCs (gray), Py230^{mCherry} cells (red), and Py230^{mCherry} and WBC mixture. The graph depicts the absence of Py230^{mCherry} cells in the whole blood 6 hours after the biopsy. Representative flow cytometry gating indicates the absence of Py230^{mCherry} cells in the peripheral blood regardless of biopsy.
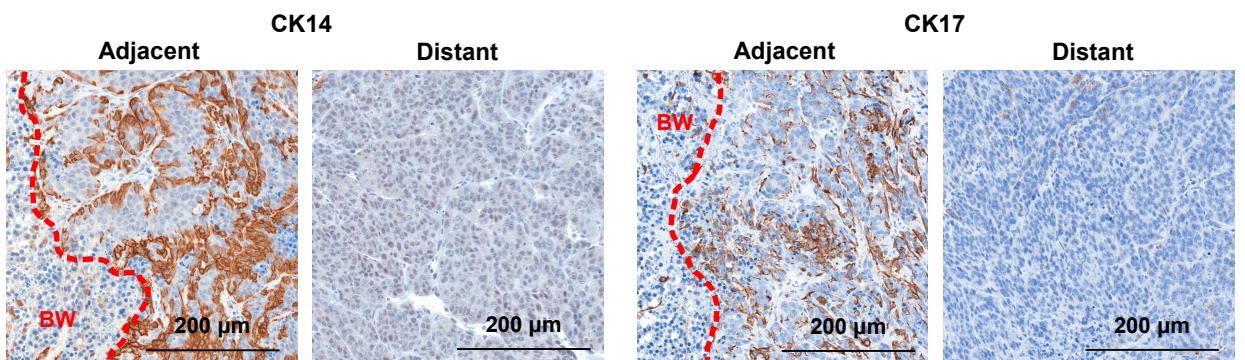
Figure S2

A

25-day post-biopsy surgical resected clinical BC
(whole mount)

Matched biopsy

Distant

Adjacent

BW

2 mm

3 mm

200 µm

200 µm

B

15-day post-biopsy Py230 tumor
(whole mount)

Matched biopsy

BW

1 mm

200 µm

C

15-day post-biopsy Py230 tumor

CK14

CK17

Adjacent

Distant

Adjacent

Distant

BW

BW

200 µm

200 µm

200 µm

200 µm

Brown: anti-CK14 or anti-CK17 Blue: hematoxylin

Figure S2. Prolonged retention of inflammatory cells adjacent to biopsy wound, related to Figure 2.
(A) Representative H&E image shows the whole mount of surgically resected tumor and the matched biopsy of tumor used for Fig. 2A. The white dotted line indicates the border of the biopsy wound (BW). High-power magnification images of adjacent and distant areas correspond to fluorescent images shown in 2A. (B) H&E image of 15-day post-biopsy Py230 tumor and vertical section of the matched biopsy used for Fig. 2D. The white dotted line indicates the border from the biopsy wound (BW). (C) Immunohistochemical staining of CK14 and CK17 (brown) in 15-day post-biopsy Py230^{mCherry} tumors both adjacent (left) to and distant (right) from the biopsy wound. Red dotted line indicates the border of biopsy wound (BW).
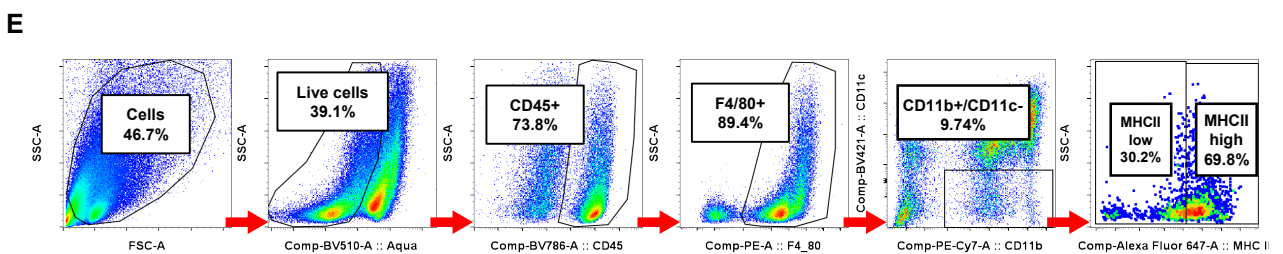
Figure S3

A

F4/80 | Biopsy(-) Parenchyma | Biopsy(+) Distant | Biopsy(+) Adjacent

Mark-up image

50 µm

F4/80 (% of total cell count)

P<0.001

Dist   Adja

Yellow: Cytoplasm **Navy:** F4/80 Positive **Light blue:** F4/80 Negative

CD206 | Biopsy(-) Parenchyma | Biopsy(+) Distant | Biopsy(+) Adjacent

Mark-up image

50 µm

CD206 (% of total cell count)

P<0.001

Dist   Adja

Yellow: Cytoplasm **Navy:** CD206 Positive **Light blue:** CD206 Negative

B

Primary MΦ

150 µm

SSC-A / FSC-A 96.7%

SSC-A / Comp-Zombie Aqua-A :: live_dead Live 97.6%

SSC-A / Comp-PE-Cy7-A :: CD45 CD45+ 99.5%

Comp-FITC-A :: CD11b / Comp-PE-A :: F4_80 F480+/CD11b+ 99.7%

C

H&E

2 mm

DsRed
DAPI

2 mm

200 µm

200 µm

D

1 mm

CD206   50 µm

Overlay   50 µm

10 µm

DsRed   50 µm

DAPI   50 µm

E

SSC-A / FSC-A Cells 46.7%

SSC-A / Comp-BV510-A :: Aqua Live cells 39.1%

SSC-A / Comp-BV786-A :: CD45 CD45+ 73.8%

SSC-A / Comp-PE-A :: F4_80 F4/80+ 89.4%

Comp-BV421-A :: CD11c / Comp-PE-Cy7-A :: CD11b CD11b+/CD11c- 9.74%

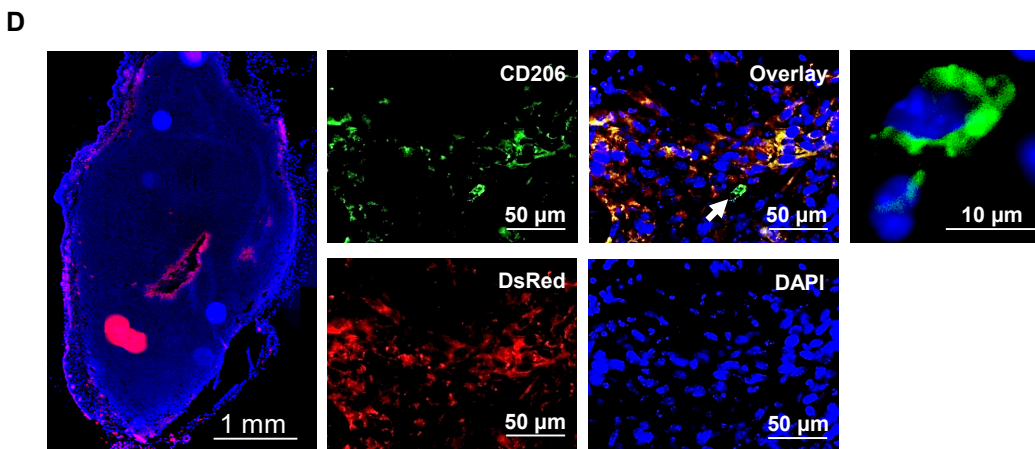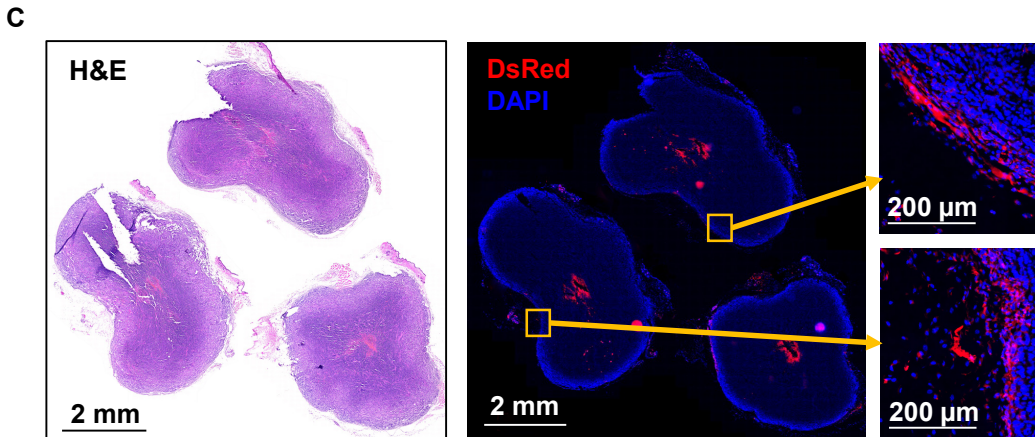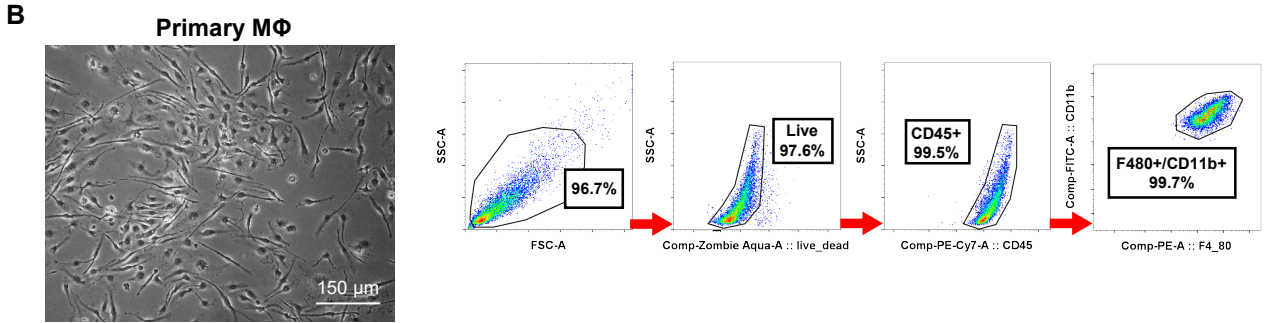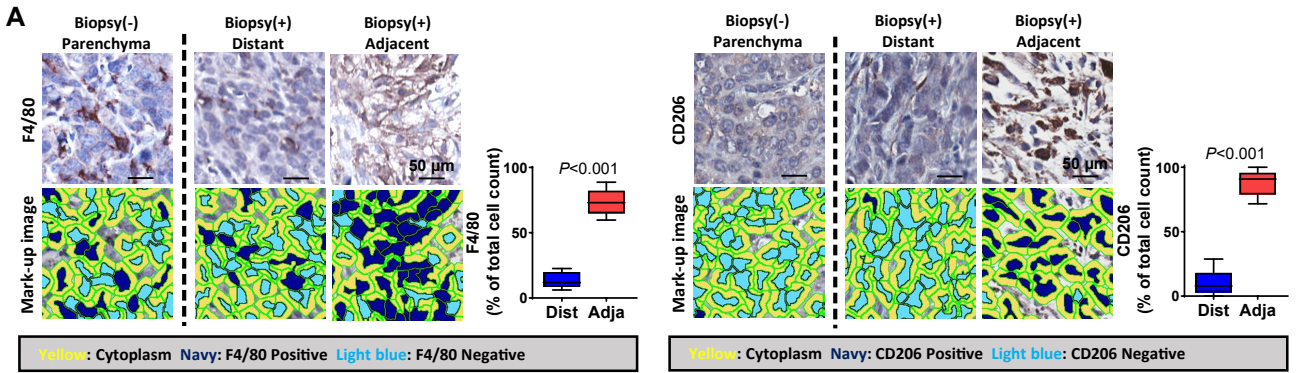SSC-A / Comp-Alexa Fluor 647-A :: MHC II MHCII low 30.2% MHCII high 69.8%

Figure S3. M2ϕ accumulation emerged as early as one day after biopsy in Py230 tumors, related to Figure 3.
(A) Algorithm used for the quantification of F4/80+ and CD206+ IHC-stained cells using Aperio Image Suite. Representative images of F4/80 and CD206 expression in unbiopsied Py230 tumor (left), distant from biopsy wound (middle), and adjacent to biopsy wound (right). Graphs depict the percentage of positive cells normalized by nucleus count (n=13). *P*-values were calculated using Wilcoxon test. (B) Brightfield image of bone marrow-derived primary Mϕ isolated from B6 female mice. Flow cytometry gating of bone marrow-derived primary Mϕ^{DsRed}. (C) Scanned image of 1-day post-biopsy Py230 tumors of mice that received Mϕ^{DsRed} adoptive transfer. The whole mount of three independent tumor images shows local accumulation of Mϕ^{DsRed} (red) around the biopsy wound (center hollow), nuclear counterstain with DAPI (blue), and corresponding H&E image. High-power images corresponding to orange squares indicate Mϕ^{DsRed} infiltration into the distant peripheral stroma. (D) Images of biopsied Py230 tumors in mice that received Mϕ^{DsRed} adoptive transfer, immunofluorescently stained with FITC-labeled anti-CD206 (green) and counterstained with DAPI (blue). White arrow indicates CD206+/mCherry- cells. BW: biopsy wound. (E) Flow cytometry gating of Mϕ immune-profiling for M1ϕ: CD45$^+$F4/80$^+$CD11b$^+$/CD11c$^-$MHC^{high} and M2ϕ: CD45$^+$F4/80$^+$CD11b$^+$/CD11c$^-$MHCII^{low}.
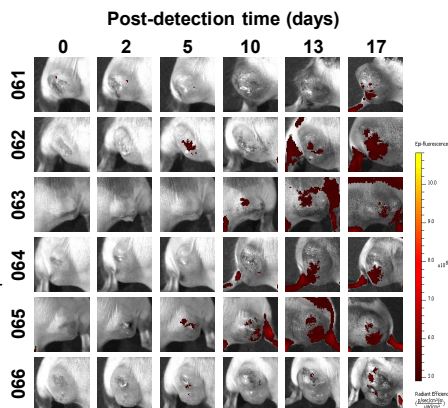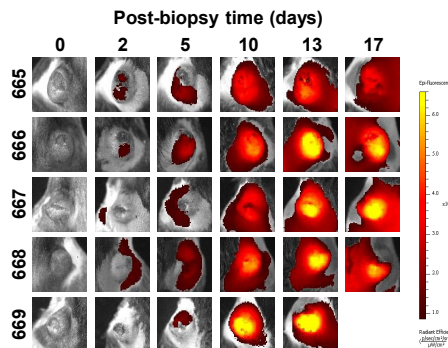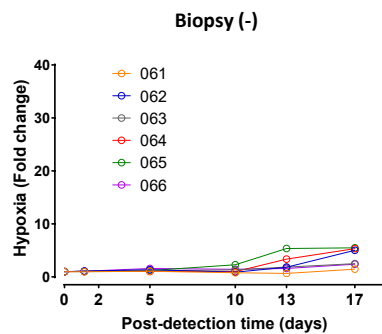
Figure S4
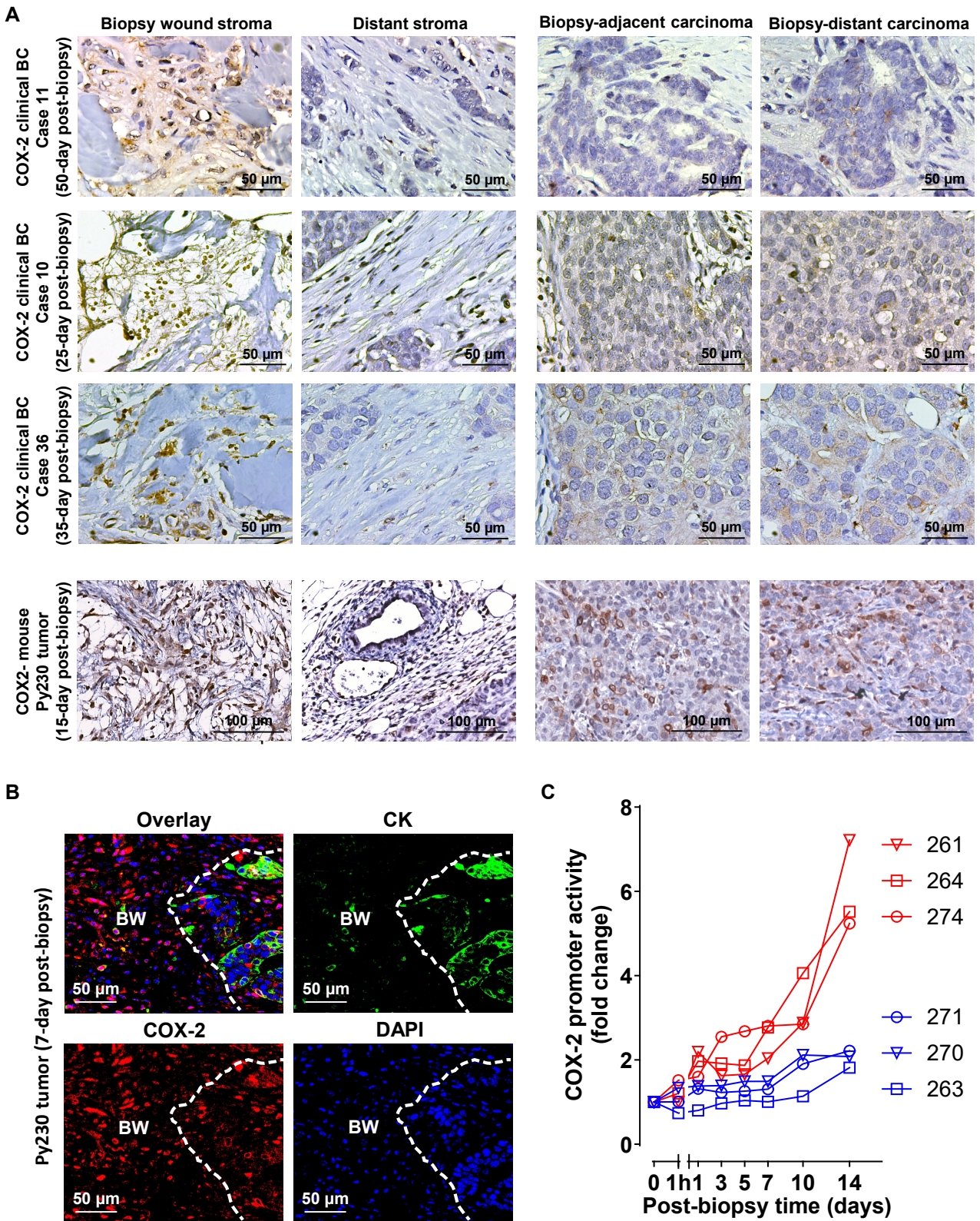
Figure S4. Sustained COX-2 activation in stromal cells in the biopsy wound, related to Figure 4.
(A) IHC staining images of COX-2 in biopsy wound stroma, peripheral stroma, carcinomas adjacent and distant from biopsy wound of three independent Stage I ER+ BC cases and 15-day post-biopsy Py230 tumor. (B) Multi-color immunofluorescent staining for CK (green), COX-2 (red), and DAPI (blue) of biopsied Py230 tumor. The white line depicts the border of biopsy wound (BW). (C) COX-2 promoter activity of individual mice before and after biopsy (red) and time-matched unbiopsied (blue) mice (n=3).

Figure S5

A
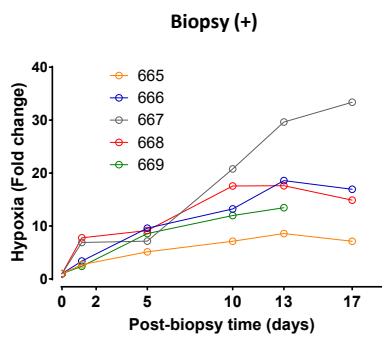
B
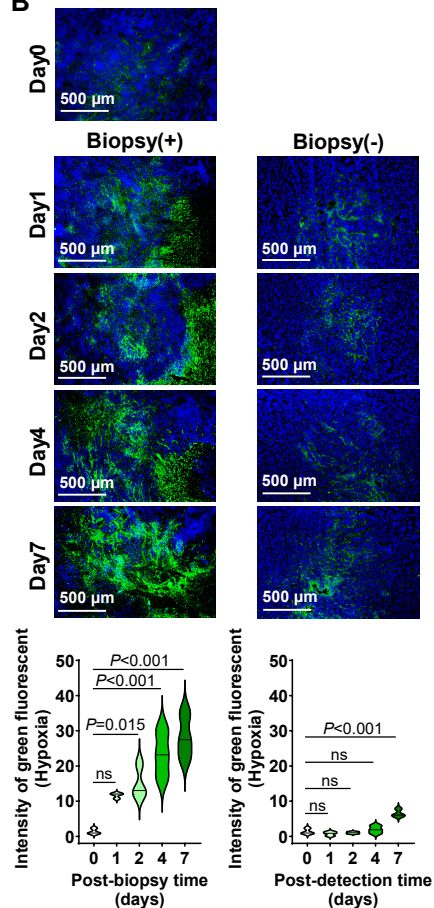
C

D

E

Figure S5. Biopsy of tumor instigates spatially limited but prolonged hypoxia, related to Figure 5.
(A) Hypoxia was measured at the indicated time after biopsy following the intravenous injection of HypoxySense®
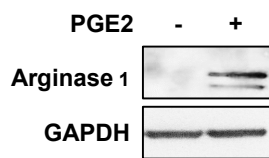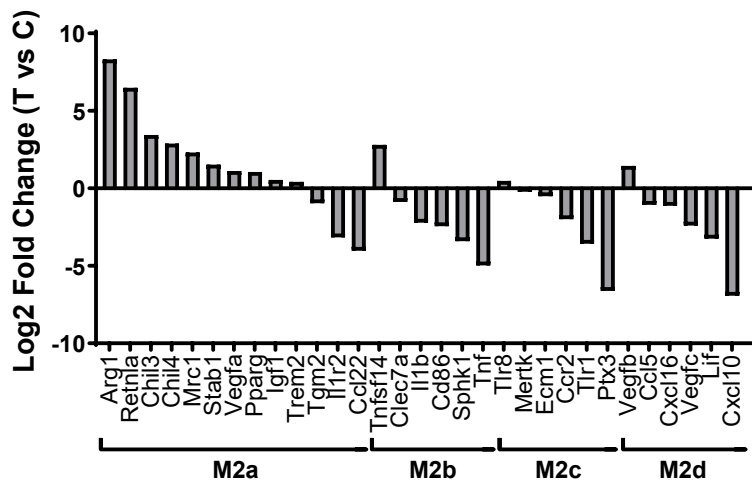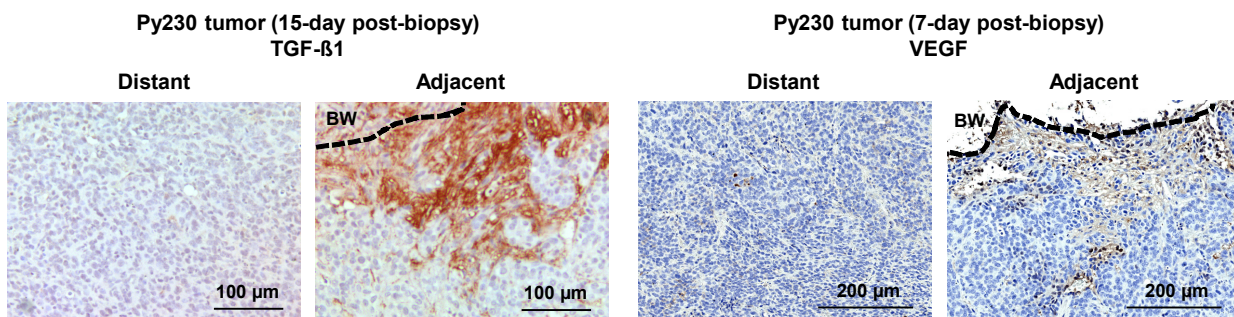using IVIS imaging system. The graph depicts fold change of photons at each time point over time 0 (before biopsy)
from individual tumors assigned to biopsy or unbiopsied control groups (n=6-7). Fluorescent images at the indicated
time points show a flux of biopsied and unbiopsied tumors. (B) Images of biopsied Py230 tumors
immunofluorescently stained for pimonidazole. Mice assigned to biopsy or unbiopsied groups were injected with
pimonidazole HCL 2 h before tumor resection. Frozen sections were immunofluorescently stained following the
vendor's instructions (n=3). The graph depicts the quantification of hypoxia measured by pixel count normalized by
area using Image J software. P-values were calculated using one-way ANOVA, relative to time 0. (C) Western blot
of Arginase-1 from Mϕ treated with or without PGE$_2$. (D) Differential gene expression comparison of M2 subtype
associated transcripts in B6 mouse Mϕ polarized by PGE$_2$ for 24 h under hypoxia over control. The Y-axis of the bar
graph indicates the log2 fold changes of M2 subgroups associated genes in B6 mouse Mϕ polarized by PGE$_2$ for 24
h under hypoxia over control. The selected genes associated with each subtype were reported in mouse
(PMID3527030, 27683760, 27474165, 28402847, 37566293, 22730547, 32642590, 23684988). Retnla, Chil3, Chil4,
and Mrc1 results were confirmed by qRT-PCR (n=3-5) due to lower sensitivity of RNA-seq. For all transcript changes
shown, P-values <0.05. (E) IHC staining for VEGF and TGF-β1 of 7-day and 15-day post-biopsy Py230 tumors. The
black dotted line depicts the border from the biopsy wound.

Figure S6

A

B

C
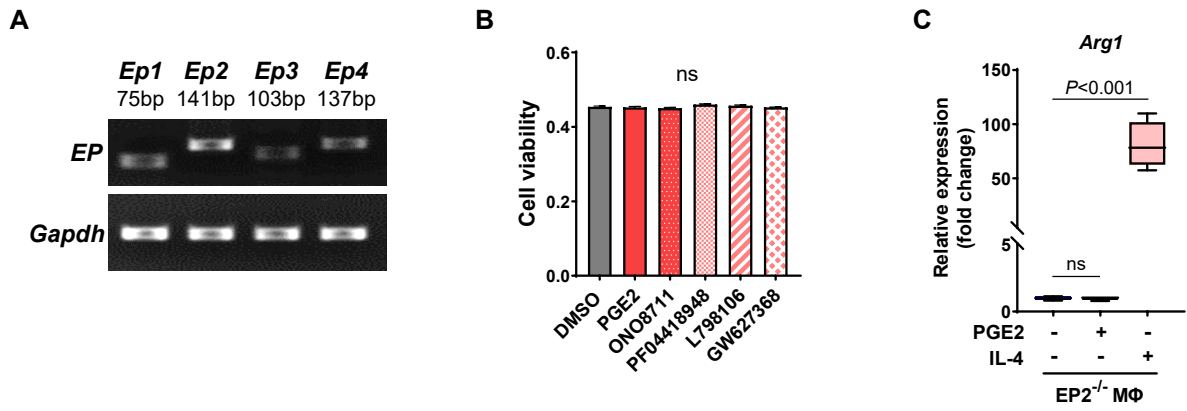
Figure S6. Absence of PGE₂-mediated M2-shift in EP2-/- Mφ, related to Figure 6.
(A) RT-qPCR analysis for mRNA expression of prostanoid receptors (*Ep1-Ep4*) in bone marrow-derived primary Mφ isolated from B6 mice. (B) MTT proliferation assay of Mφ treated with EP receptor selective antagonist at a concentration of 10 nM of ONO8711 (EP1), 1 µM of PF04418948 (EP2), 10 nM of L798106 (EP3), 1 µM of GW627368X (EP4) for 24h (n=5). Data were analyzed by one-way ANOVA, relative to untreated control. (C) RT-qPCR analysis of *Arg1* expression of *Ep2⁻/⁻* Mφ treated with PGE₂ or interleukin 4 (IL4) (n=3). *P*-values were calculated using one-way ANOVA, relative to control.

Figure S7

A

B
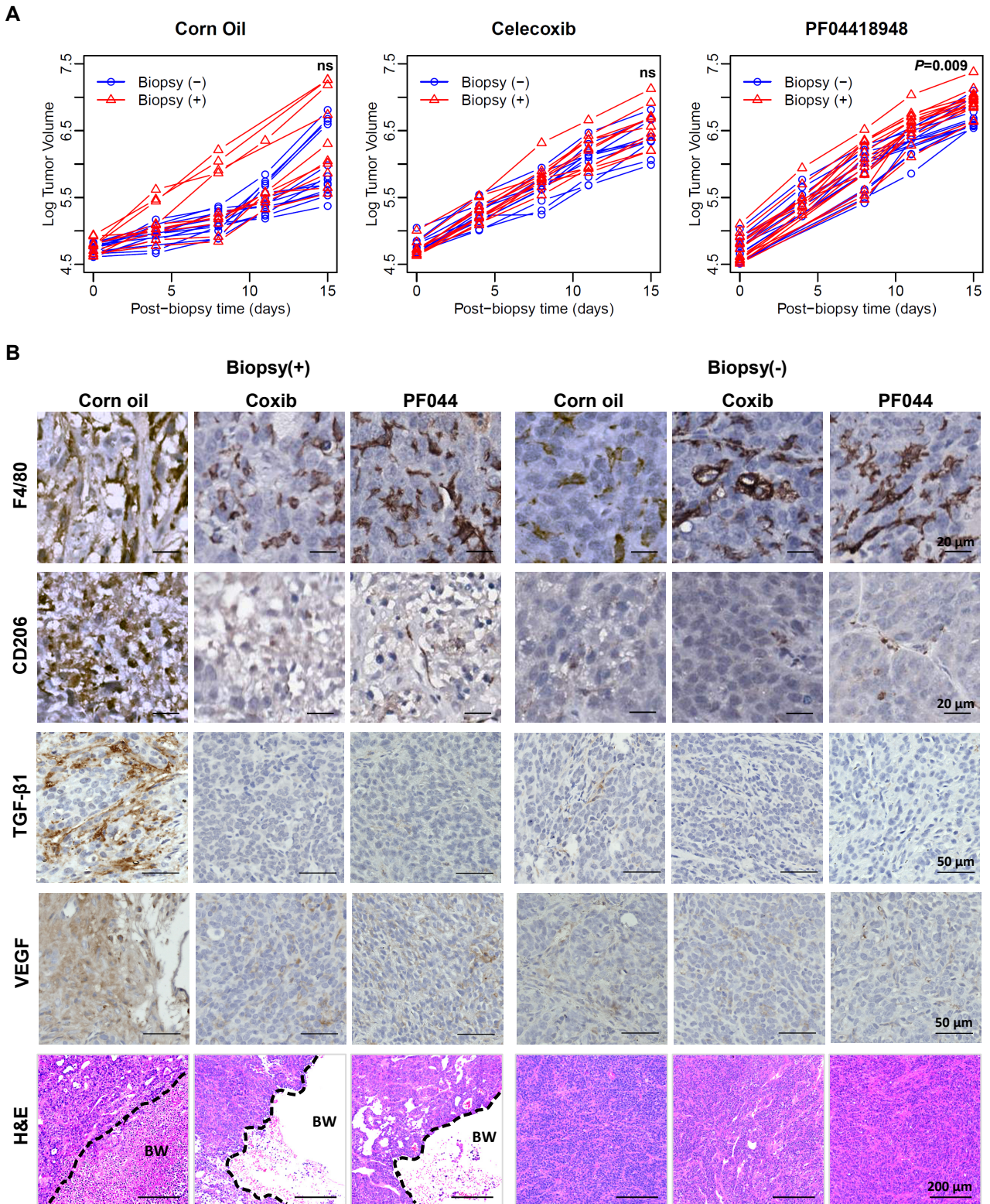
Figure S7. Oral administration of NSAIDs after biopsy inhibits biopsy-induced M2-polarization, related to Figure 7.
(A) Py230^{mCherry} tumor growth rate in mice assigned to experiments corresponding to Fig. 7A. One day after the biopsy, the mice were orally administered with either corn oil (control, n=10-11), celecoxib (n=10), or PF04418948 (n=13-15) in food *ad libitum*. The tumor volume of each mouse was plotted over post-biopsy days (biopsy as day 0). *P*-values at study endpoint were calculated using Student's T-test. (B) IHC staining images for F4/80, CD206, TGF-β1, VEGF (brown), and Hematoxylin counterstaining (blue). H&E images of biopsied or unbiopsied tumors derived from mice administered with corn oil, celecoxib, or PF04418948. The black dotted line indicates the border of the biopsy wound. BW: biopsy wound.

Table S1

```
┌─────────────────────────────────────────────────────────────────────────┐
│         Breast cancer patients, NCDB, 2004-2017 (n=2,981,732)             │
└─────────────────────────────────────────────────────────────────────────┘
                                    ↓
┌─────────────────────────────────────────────────────────────────────────┐
│         Breast cancer 1st and only cancer (n=2,220,634)                   │
└─────────────────────────────────────────────────────────────────────────┘
```

Exclusions:
  Male (n=19,332)
  Clinically or pathologically DCIS/LCIS or III-IV (n=1,089,951)
  Non-invasive or inflammatory histology (n=1,649)
  Diagnosis and all or part of treatment at facility other than reporting (n=572,778)
  No/missing biopsy or same day surgery (n=84,418)
  Discordant hormone receptor and endocrine treatment status (n=2,111)
  Neoadjuvant or non-definitive surgery as first treatment (n=98,032)
  No adjuvant treatment or first adjuvant treatment > 1 year post-surgery (n=16,390)
  Did not receive recommended adjuvant therapies due to contraindications or choice (n=58,510)
  Age $\geq$80 years old (n=21,194)
  Missing demographic information (n=52,864)
  Missing treatment information (n=2,244)
  No follow-up information (i.e. 2017 diagnoses; n=22,498)
  TTS =7 and >356 (n=2,200)

```
┌─────────────────────────────────────────────────────────────────────────┐
│         Clinical Stage I-II, adjuvant treated patients (n= 176,481)       │
└─────────────────────────────────────────────────────────────────────────┘
```
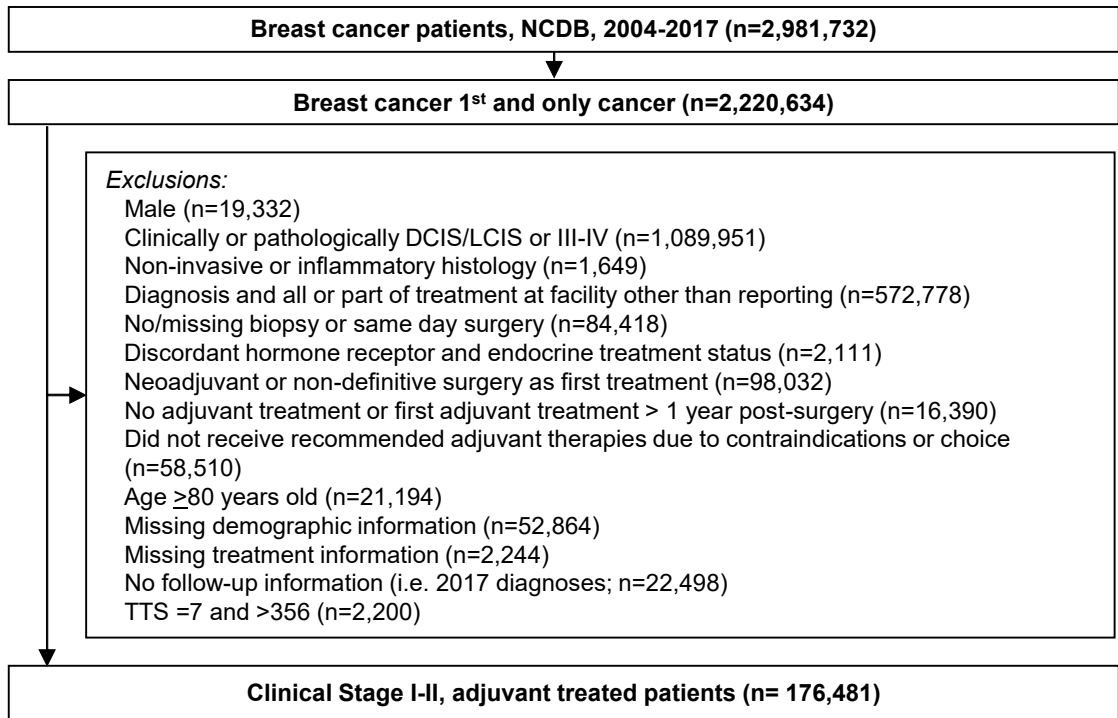
Table S2

Table S2. Median and Quartiles of biopsy-to-surgery interval (days) by demographic and clinical characteristics of the cohort, related to Figure 1.

	N (%)	Q1	Median	Q3
Overall	176481 (100)	20	28	41
Age				
<30	587 (0.33)	19	29	41
30-39	5815 (3.29)	20	29	43
40-49	28895 (16.37)	20	30	43
50-59	48421 (27.44)	20	28	41
60-69	56535 (32.03)	20	28	41
≥70	36228 (20.53)	20	28	40
Race				
White	143848 (81.51)	20	28	40
Hispanic	8523 (4.83)	24	35	51
Black	17882 (10.13)	22	34	49
Other	6228 (3.53)	21	31	45
Comorbidity				
0	147363 (83.50)	20	28	41
1	23383 (13.25)	20	29	42
=2	5735 (3.25)	21	31	44
Year of Diagnosis				
2004	3835 (2.17)	15	22	33
2005	4444 (2.52)	16	23	34
2006	5357 (3.04)	16	23	34
2007	6640 (3.76)	18	27	38
2008	12434 (7.05)	18	27	39
2009	15300 (8.67)	19	28	39
2010	15165 (8.59)	19	28	40
2011	16763 (9.50)	20	28	40
2012	16906 (9.58)	20	29	42
2013	17769 (10.07)	21	29	42
2014	19691 (11.16)	21	30	43
2015	20796 (11.78)	21	31	44
2016	21381 (12.12)	22	31	44
Clinical Stage[a]				
I	132865 (75.29)	20	28	41
II	43616 (24.71)	20	29	42
Histology Type				
Ductal	144283 (81.76)	20	28	41
Lobular	14316 (8.11)	21	31	44
Ductal and Lobular	9174 (5.20)	21	30	43
Other	8708 (4.93)	20	28	41
Histology Grade				
1	50553 (28.65)	20	29	41
2	79348 (44.96)	20	29	42
>3	46580 (26.39)	19	28	40
Type of Surgery				
Breast Conserving	125297 (71.00)	19	27	38
Mastectomy	31554 (17.88)	20	29	42
Mastectomy with Reconstruction	19630 (11.12)	28	40	54
Urban/Rural Status[b]				
Metro ≥ 1 million	90102 (51.05)	21	30	43
Metro < 1 million	60932 (34.53)	19	28	40
Urban/Rural	25447 (14.42)	17	26	36
Endocrine Therapy				
No	29983 (16.99)	19	27	39
Yes	146498 (83.01)	20	29	42
Chemotherapy/Biological				
No	104659 (59.30)	20	29	42
Yes	71822 (40.70)	19	28	40
Radiation Therapy				
No	51608 (29.24)	22	33	47
Yes	124873 (70.76)	19	27	39
Hormone Receptor				
Positive	154126 (87.33)	20	29	42
Negative	22355 (12.67)	18	27	38
Type of First Adjuvant Therapy				
Radiation	64470 (36.53)	31	42	55
Chemotherapy/BRM	67478 (38.24)	30	40	51
Endocrine Therapy	44533 (25.23)	21	33	48
Insurance type				
Not Insured	3372 (1.91)	22	34	52
Private Insurance	101483 (57.50)	20	28	41
Medicaid	10357 (5.87)	22	34	50
Medicare	52719 (29.87)	20	28	40
Other Government	8550 (4.84)	21	30	44
% No High School Degree[c]				
≥ 29%	24212 (13.72)	21	30	45
20-28.9%	36578 (20.73)	20	29	42
14-19.9%	41417 (23.47)	20	28	41
< 14%	74274 (42.09)	20	28	40
Median Income[c]				
< $30,000	18613 (10.55)	20	29	43
$30,000 – $34,999	27939 (15.83)	19	28	41
$35,000 – $45,999	48698 (27.59)	20	28	41
> $46,000	81231 (46.03)	20	29	41

a. Clinical Group Stage derived from AJCC 6th or 7th ed. Staging Manual. b. Urban/Rural Status derived from the 2000 USDA Economic Research Service Urban-Rural continuum codes. c. Education (% no high school degree) and median income quartiles for patient's ZIP-code of residence at time of diagnosis derived from year 2000 US Census data.

Table S3

A. EMT histologic analyses

Total case	12
Preoperative interval	29.4 (12-54)
Age	62.9 ± 9.7
Race	
White	9
Other	2
Unknown	1
pT	
I	10
II	2
pN	
Negative	9
Positive	3
Grade	
I	3
II	5
III	4
Luminal	
A	8
B	4

B. M2Φ histologic analyses

Total case	14
Preoperative interval	28.8 (10-54)
Age	63.1 ± 10.1
Race	
White	11
Other	2
Unknown	1
pT	
I	12
II	2
pN	
Negative	12
Positive	2
Grade	
I	4
II	7
III	3
Luminal	
A	11
B	3

Table S4

RT-qPCR				
Gene	Forward Primer (5'-3')	Reverse Primer (5'-3')	Size (bp)	Tm (°C)
Arg1	CTTGCGAGACGTAGACCCTG	GCCAATCCCCAGCTTGTCTA	94	57.3
Ym1	TCATTACCCTGATAGGCATAGG	TTATCCTGAGTGACCCTTCTAAG	184	53.4
Ym2	GCTGGACCACCAGGAAAGTA	TCAGTGGCTCCTTCATTCAGA	86	55.8
LIGHT	CTGCATCAACGTCTTGGAGA	GATACGTCAAGCCCCTCAAG	205	57.9
Fizz-1	GGTCCCAGTGCATATGGATGAGACCATAGA	CACCTCTTCACTCGAGGGACAGTTGGCAGC	296	67.0
CD206	GGATTGCCCTGAACAGCAAC	ACTTAAGCTTCGGCTCGTCA	102	59.7
Gapdh	AGGTCGGTGTGAACGGATTTG	TGTAGACCATGTAGTTGAGGTCA	123	55.1

Genotyping					
Target	Name	Forward Primer (5'-3')	Reverse Primer (5'-3')	Size (bp)	Tm (°C)
COX-2	Mutant	CCATTAGCAGCCAGTTGTCA	AGCCTTATGCAGTTGCTCTC	225	F:58.2 R:58.0
	Wild type	CCATTAGCAGCCAGTTGTCA	TGCTAGAAAGGGGGTCTGAG	245	F:58.2 R:58.4
EP2	Mutant	ATTAAGGGCCAGCTCATTCC	CGTACTCCCCGTAGTTGAGC	300	F:57.6 R:59.9
	Wild type	TGCTCATGCTCTTCGCTATG	CGTACTCCCCGTAGTTGAGC	165	F:58.1 R:59.9